

ELECTRONIC SUPPORTING INFORMATION

Bifunctional heterobimetallic 3d-4f [Co(II)-RE, RE = Dy, Eu, Y] ionic complexes: modulation of the magnetic-luminescent behaviour

Matteo Bombaci,^a Francesca Lo Presti,^a Anna L. Pellegrino,^a Martina Lippi,^b Patrizia Rossi,^b Leonardo Tacconi^c, Lorenzo Sorace,^{c,*} and Graziella Malandrino^{a,*}

a) *Dipartimento Scienze Chimiche, Università degli Studi di Catania, and INSTM UdR Catania, Viale Andrea Doria 6, 95125 Catania, Italy*

b) *Dipartimento di Ingegneria Industriale, Università degli Studi di Firenze, Via Santa Marta 3, 50136 Firenze, Italy*

c) *Dipartimento di Chimica "U. Schiff", Università degli Studi di Firenze, and INSTM UdR Firenze, Via della Lastruccia 3, 50019 Sesto Fiorentino (FI), Italy*

Table of contents

Table S1. Selected bond lengths and angles in **Eu-Co** and **Y-Co** complexes.

Fig. S1. Stick view of the [Y(hfa)₂tetraglyme]⁺ cation in **Y-Co** complex.

Fig. S2. Stick view of the Co(hfa)₃⁻ anion in **Y-Co** complex.

Fig. S3. PXRD patterns of **Dy-Co** (black, experimental), **Eu-Co** (red, experimental) and **Y-Co** (blue, experimental).

Fig. S4. FT-IR spectra of the **Dy-Co**, **Eu-Co** and **Y-Co** complexes.

Table S2 SHAPE parameters for the coordination sphere of Cobalt(II) in Y-Co and (NEt₄)Co(hfa)₃ (ref. 1).

Fig. S5. Coordination environment of the Co(II) centre in the two complexes: **a)** Et₄N[Co^{II}(hfa)₃]; **b)** YCo.

Table S3 Co-O bond distances in the Co(II) coordination environment for the two complexes.

Fig. S6. Comparison of the relaxation rate observed for **Y-Co** under an external applied field of 1.2 KOe and for **Dy-Co**.

Fig. S7. Emission spectra, recorded at room temperature, with an excitation wavelength of 310 nm for the **Dy-Co** solution (CH₂Cl₂) and **Dy-Co** powder film obtained through drop-casting on quartz.

Supplementary Note S1. Fitting procedure of experimental DC magnetometry data and g factors.

References

Table S1. Selected bond lengths (Å) and angles (°) in **Eu-Co** and **Y-Co**.

M (Eu in Eu-Co and Y in Y-Co)		Co	
	Eu-Co / Y-Co		Eu-Co / Y-Co
M1-O1D	2.392(2) / 2.345(2)	Co1-O1A	2.058(2) / 2.058(2)
M1-O2D	2.378(2) / 2.333(2)	Co1-O2A	2.059(2) / 2.058(2)
M1-O1E	2.376(2) / 2.328(2)	Co1-O1B	2.060(2) / 2.060(3)
M1-O2E	2.423(2) / 2.375(2)	Co1-O2B	2.059(2) / 2.063(2)
M1-O3	2.524(2) / 2.492(3)	Co1-O1C	2.074(2) / 2.070(2)
M1-O4	2.473(2) / 2.428(2)	Co1-O2C	2.076(2) / 2.071(3)
M1-O5	2.487(2) / 2.450(2)		
M1-O6	2.438(2) / 2.390(2)		
M1-O7	2.512(2) / 2.475(2)		
	Eu-Co / Y-Co		Eu-Co / Y-Co
O1D-M1-O2D	70.77(7) / 71.70(8)	O1A-Co-O2A	88.71(8) / 88.6(1)
O1D-M1-O1E	140.47(7) / 139.59(8)	O1A-Co1-O1B	88.68(8) / 88.6(1)
O1D-M1-O2E	134.92(7) / 134.69(8)	O1A-Co1-O2B	176.64(8) / 176.5(1)
O1D-M1-O3	75.368(7) / 75.66(8)	O1A-Co1-O1C	86.75(8) / 86.7(1)
O1D-M1-O4	71.89(7) / 72.12(8)	O1A-Co1-O2C	92.82(8) / 93.3(1)
O1D-M1-O5	67.69(7) / 67.68(8)	O2A-Co1-O1B	91.76(8) / 91.7(1)
O1D-M1-O6	86.45(7) / 86.26(8)	O2A-Co1-O2B	93.46(8) / 93.63(9)
O1D-M1-O7	135.85(7) / 136.72(8)	O2A-Co1-O1C	173.02(8) / 172.8(1)
O2D-M1-O1E	111.01(7) / 110.60(8)	O2A-Co1-O2C	87.72(8) / 87.5(1)
O2D-M1-O2E	140.78(7) / 139.60(8)	O1B-Co1-O2B	88.69(8) / 88.65(9)
O2D-M1-O3	72.55(7) / 71.75(8)	O1B-Co1-O1C	93.43(8) / 93.64(9)
O2D-M1-O4	129.68(7) / 130.31(8)	O1B-Co1-O2C	178.40(8) / 178.0(1)
O2D-M1-O5	125.85(6) / 126.35(8)	O2B-Co1-O1C	91.33(8) / 91.36(9)
O2D-M1-O6	78.60(6) / 77.51(8)	O2B-Co1-O2C	89.84(8) / 89.55(9)
O2D-M1-O7	70.39(6) / 69.78(8)	O1C-Co1-O2C	87.22(8) / 87.28(9)
O1E-M1-O2E	69.60(7) / 70.62(8)		
O1E-M1-O3	68.08(7) / 67.74(8)		
O1E-M1-O4	79.43(6) / 78.24(8)		
O1E-M1-O5	123.14(7) / 123.05(8)		

O1E-M1-O6	133.08(7) / 134.13(8)		
O1E-M1-O7	74.30(7) / 73.91(8)		
O2E-M1-O3	134.21(7) / 135.56(8)		
O2E-M1-O4	89.49(6) / 90.02(8)		
O2E-M1-O5	67.23(6) / 67.01(8)		
O2E-M1-O6	75.26(6) / 75.39(8)		
O2E-M1-O7	72.46(6) / 72.26(8)		
O3-M1-O4	66.40(6) / 67.14(8)		
O3-M1-O5	125.90(6) / 126.82(8)		
O3-M1-O6	149.72(6) / 147.90(8)		
O3-M1-O7	111.17(6) / 109.41(8)		
O4-M1-O5	65.18(6) / 65.75(8)		
O4-M1-O6	130.85(6) / 132.03(8)		
O4-M1-O7	151.98(6) / 150.66(8)		
O5-M1-O6	65.83(6) / 66.48(8)		
O5-M1-O7	122.89(6) / 123.74(8)		
O6-M1-O7	66.01(6) / 66.91(8)		

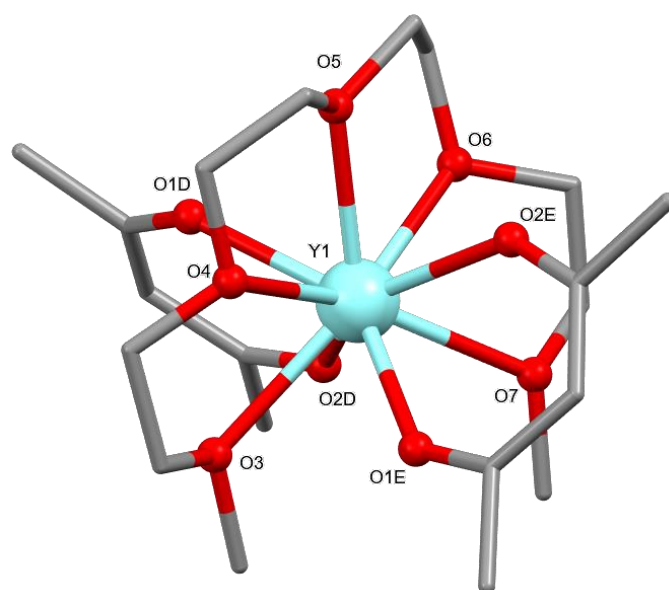


Fig. S1. Ball and stick view of the structure of $[\text{Y}(\text{hfa})_2\text{tetraglyme}]^+$ cation in **Y-Co**; hydrogen and fluorine atoms have been omitted for sake of clarity.

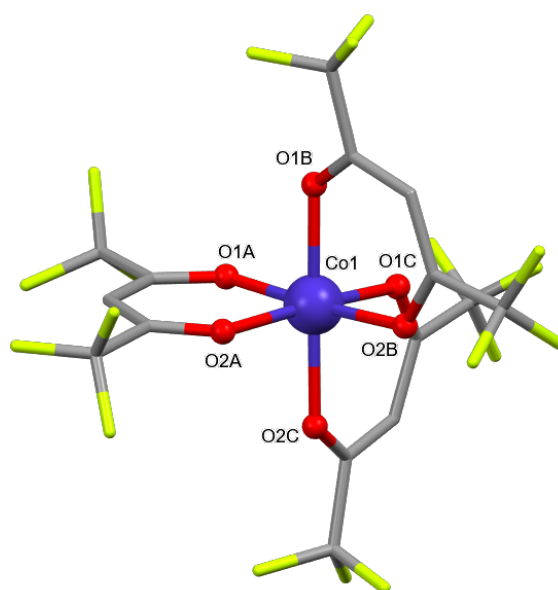


Fig.S2. Ball and stick view of the structure of $\text{Co}(\text{hfa})_3^-$ anion of **Y-Co**, hydrogen atoms have been omitted for sake of clarity.

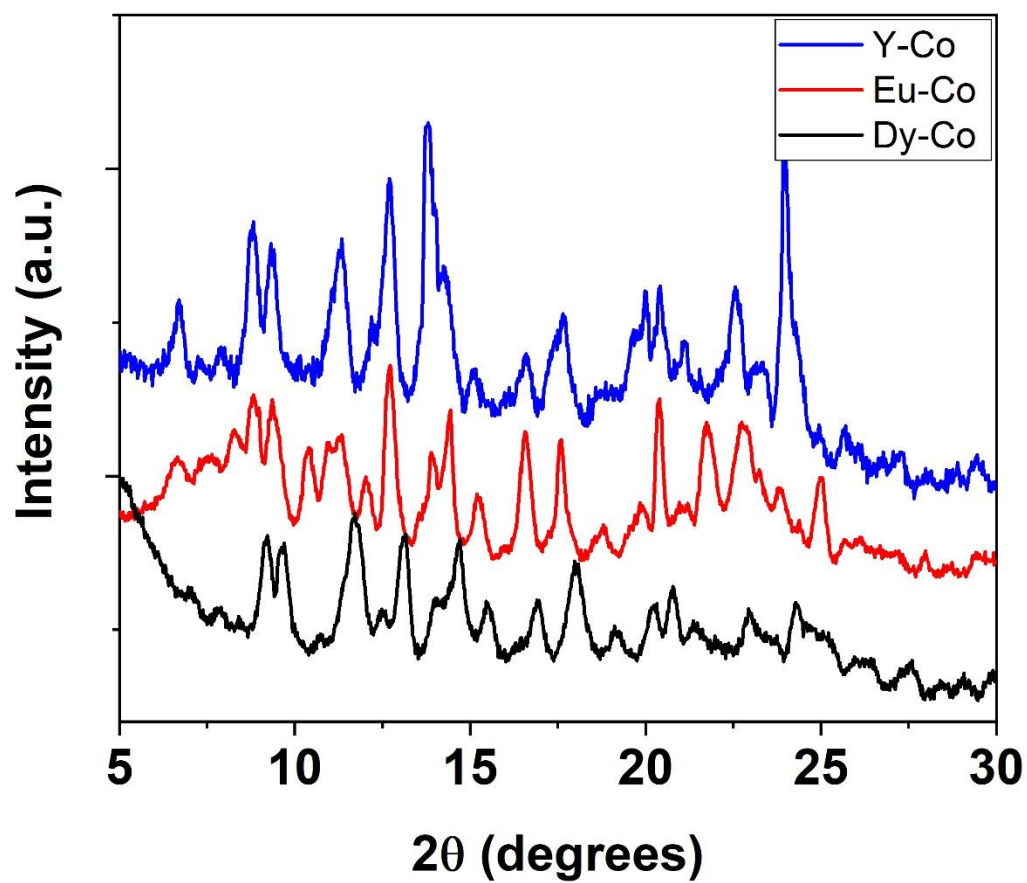


Fig. S3. PXRd patterns of **Dy-Co** (black, experimental), **Eu-Co** (red, experimental) and **Y-Co** (blue, experimental).

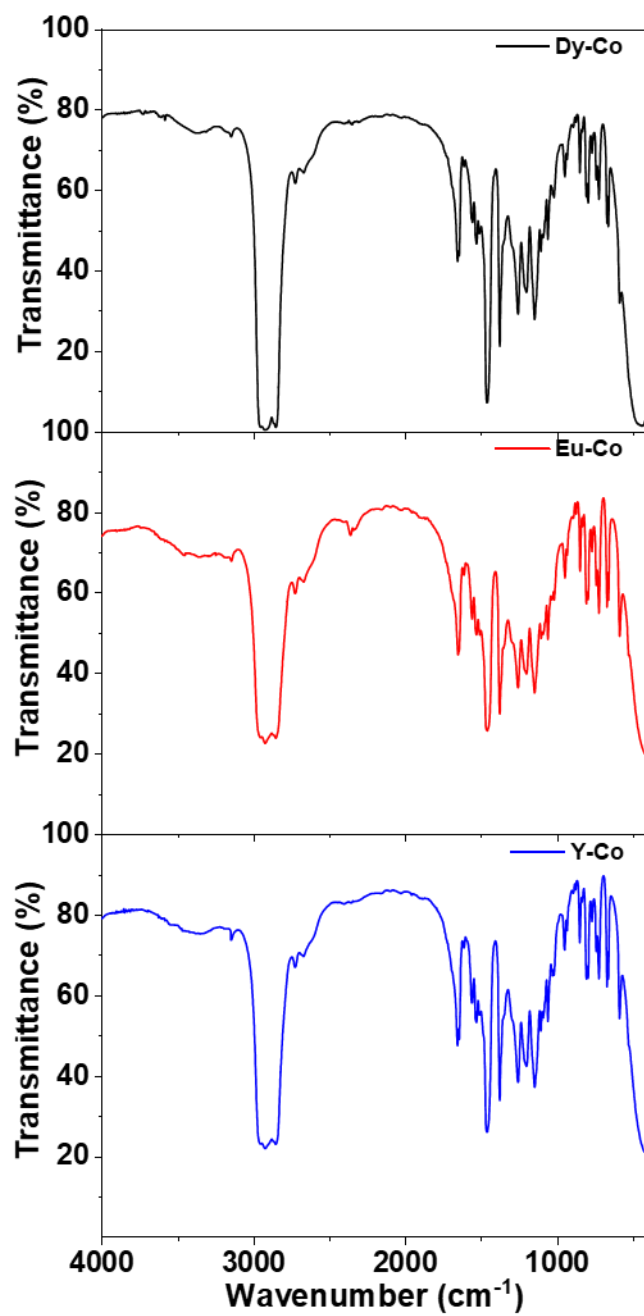


Fig.S4. FT-IR spectra of the Y-Co, Dy-Co and Eu-Co complexes.

	HP-6 Hexagon (D _{6h})	PPY-6 Pentagonal pyramid C _{5v}	OC-6 Octahedron O _h	TPR-6 Trigonal prism D _{3h}	JPPY-6 Johnson pentagonal pyramid J2 C _{5v}
Et ₄ N[Co ^{II} (hfa) ₃]	32.862	27.854	0.181	14.538	31.583
Y-Co	32.878	27.371	0.169	14.129	31.090

Table S2 SHAPE parameters for the coordination sphere of Cobalt(II) in Y-Co and (NEt₄)Co(hfa)₃ (ref. 1).

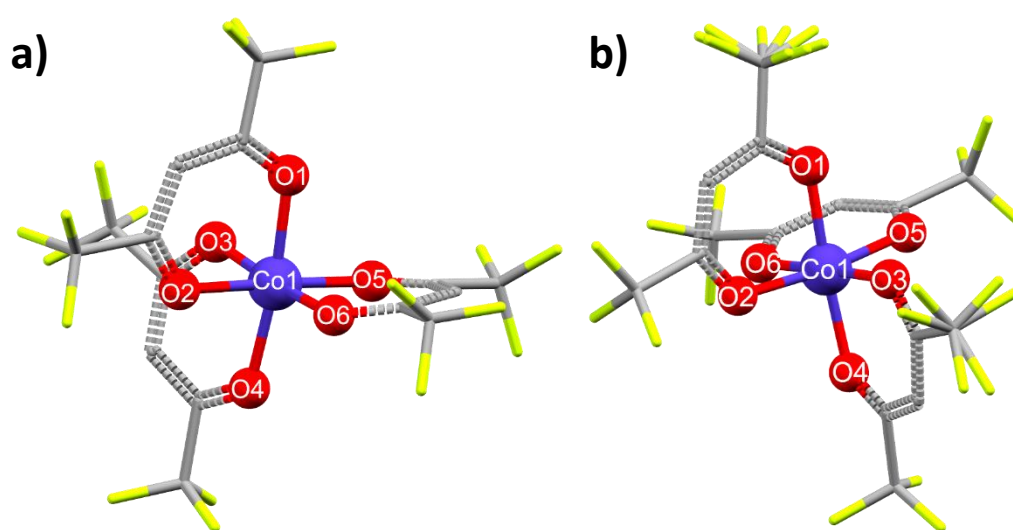


Fig. S5. Coordination environment of the Co(II) centre in the two complexes: **a)** Et₄N[Co^{II}(hfa)₃]; **b)** Y-Co.

Bond distances (Å)			
Et ₄ N[Co ^{II} (hfa) ₃]		YCo	
Co1 – O1	2.077(2)	Co1 – O1	2.058(2)
Co1 – O2	2.078(2)	Co1 – O2	2.058(2)
Co1 – O3	2.053(1)	Co1 – O3	2.060(2)
Co1 – O4	2.084(2)	Co1 – O4	2.063(2)
Co1 – O5	2.077(2)	Co1 – O5	2.071(2)
Co1 – O6	2.047(1)	Co1 – O6	2.070(2)

Table S3 Co-O bond distances in the Co(II) coordination environment for the two complexes.

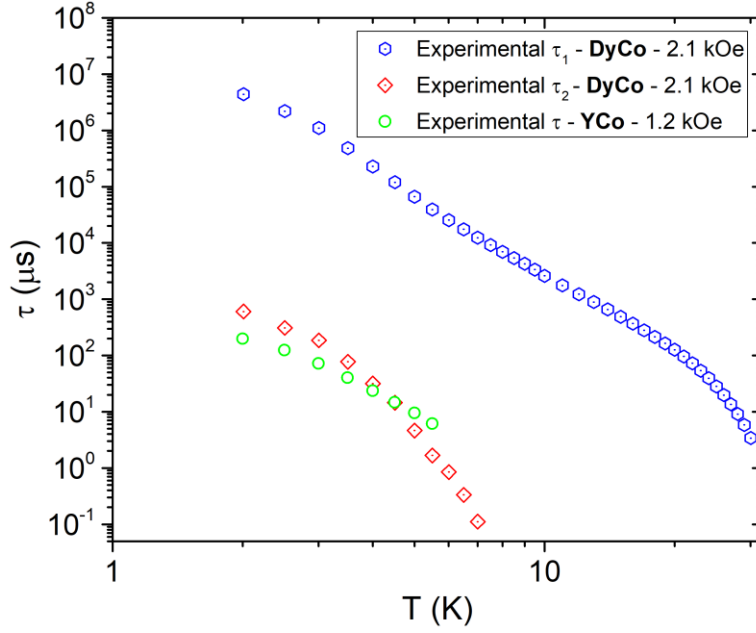


Fig. S6. Comparison of the relaxation rate observed for **Y-Co** under an external applied field of 1.2 kOe and for **Dy-Co** in an applied field of 2.1 kOe.

Supplementary Note S1. Fitting procedure of experimental DC magnetometry data and g factors.

The fitting procedure was conducted with a custom-written MATLAB script based on the toolkit EASYS PIN and the *fminuit* minimization routine. The goodness of fit between the experimental data and the simulated ones was evaluated as the coefficient of determination R^2 (worst value = $-\infty$, best value = +1) (ref. 2).

$$R^2 = 1 - \frac{\sum_{i=1}^m (Y_i - \bar{Y})^2}{\sum_{i=1}^m (Y_i - X_i)^2}$$

In this equation Y_i , \bar{Y} and X_i represent the experimental data set, the averaged value of the experimental data set and the simulated dataset.

Since *fminuit* is a minimization routine (i.e., it minimizes a scalar value by adjusting free parameters), the code was designed to minimize the quantity $1 - R^2$ (worst value = $+\infty$, best value = 0). The expression for it is given by:

$$1 - R^2 = \frac{\sum_{i=1}^m (Y_i - \bar{Y})^2}{\sum_{i=1}^m (Y_i - X_i)^2}$$

In this specific case, the goodness of fit was evaluated as $1 - R^2 = 0.0407$, corresponding to $R^2 = 0.9593$.

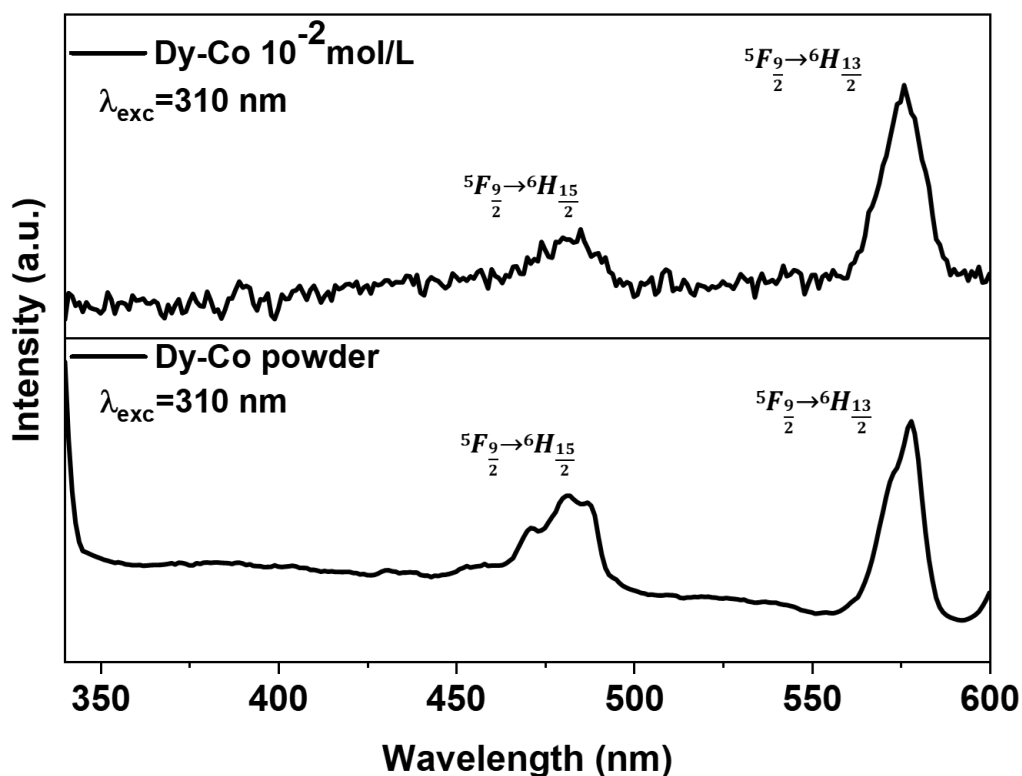


Fig. S7. Emission spectra, recorded at room temperature, with an excitation wavelength of 310 nm for the Dy-Co solution (CH_2Cl_2) and Dy-Co powder film obtained through drop-casting on quartz.

References

1. A. V. Palii, D. V. Korchagin, E. A. Yureva, A. V. Akimov, E. Ya. Misochko, G. V. Shilov, A. D. Talantsev, R. B. Morgunov, S. M. Aldoshin and B. S. Tsukerblat, *Inorg. Chem.*, 2016, **55**, 9696–9706.
2. D. Chicco D, M. J. Warrens, G. Jurman, The coefficient of determination R-squared is more informative than SMAPE, MAE, MAPE, MSE and RMSE in regression analysis evaluation. *PeerJ Computer Science*, 2021, 7:e623.